Research Square

Preprints are preliminary reports that have not undergone peer review.
They should not be considered conclusive, used to inform clinical practice,
or referenced by the media as validated information.

An explainable hierarchical machine learning framework for schizophrenia biomarker detection based on electroencephalogram signals

Mohammadreza Norouzi
University of Tehran
Fatemeh Farokhshad
Islamic Azad University
Amirhesam Ghasri
Tarbiat Modares University
Sara Bagherzadeh
Islamic Azad University
Pouya Tolou Kouroshi
Iran University of Science and Technology (IUST)
Ahmad Shalbaf
shalbaf@sbmu.ac.ir

Shahid Beheshti University of Medical Sciences

Research Article

Keywords: electroencephalogram (EEG), schizophrenia biomarker detection, SHapley Additive explanation (SHAP), machine learning, Sequential Forward Selection (SFS)

Posted Date: September 1st, 2026

DOI: https://doi.org/10.21203/rs.3.rs-10541633/v1

License: This work is licensed under a Creative Commons Attribution 4.0 International License.
Read Full License

Additional Declarations: No competing interests reported.

Abstract

Background

Schizophrenia (SZ) is a severe psychiatric disorder that requires objective biomarkers to support clinical diagnosis. Electroencephalography (EEG) provides a non-invasive and cost-effective approach for automated SZ detection; however, many previous studies have been limited by small sample sizes and suboptimal feature selection. This study utilized the ASEEG dataset comprising 101 demographically matched participants (51 SZ and 50 healthy controls). A comprehensive set of resting-state EEG features was extracted under eyes-closed (EC) and eyes-open (EO) conditions. Sequential Forward Selection (SFS) identified the optimal 20-feature subset, and ten machine learning classifiers were evaluated using leave-one-subject-out (LOSO) cross-validation. SHapley Additive exPlanations (SHAP) were employed to interpret model predictions and identify the most influential biomarkers.

Results

Under the EC condition, Random Forest and XGBoost achieved the highest classification accuracy (81.44%), with Random Forest yielding the best discrimination (AUC = 0.877). Under the EO condition, XGBoost achieved the highest accuracy (78.35%), while MLP attained the highest AUC (0.853). SHAP analysis identified permutation entropy at the frontal midline electrode Fz as the most influential feature. Additional important biomarkers included alpha-band power at the right temporal region (T4), Higuchi fractal dimension, median frequency, and gamma-band mean power at the left temporal region (T3), together with the peak ratio at the right central region (C4). These results demonstrate that combining nonlinear complexity measures with spectral EEG features improves schizophrenia discrimination.

Conclusion

The proposed framework, integrating SFS-based feature selection with explainable machine learning, achieved robust schizophrenia classification while providing interpretable EEG biomarkers. The findings highlight the complementary value of nonlinear and spectral EEG features and support the potential of explainable EEG-based models as objective tools for schizophrenia diagnosis, warranting further validation for clinical translation.

1. Introduction

Schizophrenia (SZ) is a chronic psychiatric disorder that profoundly alters thought, emotion, and behavior, often leading to social withdrawal, motivational loss, and flattened emotional expression. Affecting approximately one percent of the global population, it represents a major public health burden [1]. Currently, diagnosis remains largely dependent on clinical interviews and standardized criteria such as the Diagnostic and Statistical Manual of Mental Disorders (DSM-5) [2] or International Classification

of Diseases 10th Revision (ICD-10) [3]. However, the subjective nature of these methods contributes to diagnostic delays and misclassification, highlighting the need for objective, brain-based biomarkers.

Electroencephalography (EEG) has emerged as a particularly valuable tool in SZ research [4–7]. By capturing the brain's electrical activity with high temporal resolution, EEG enables detailed examination of neural dynamics that may reflect the underlying pathophysiology of the disorder. Unlike structural or functional MRI, EEG is cost-effective, non-invasive, and widely accessible, making it well-suited for both clinical and research applications. Given these advantages, there has been growing interest in leveraging computational approaches to extract diagnostic information from EEG signals. However, the complexity of brain electrical activity and the subtle nature of schizophrenia-related neural signatures make automated detection a challenging task [4].

Machine learning (ML) has emerged as a key tool for extracting discriminative patterns from EEG data, enabling automated construction of data models that capture knowledge hidden within complex neural signals [5]. Unlike purely manual approaches, ML algorithms learn these representations directly from extracted features, then apply the resulting models to classify new, unseen data [6]. In the context of SZ detection, recent studies have demonstrated strong ML performance across tasks including disorder classification, mechanistic interpretation, and clinical outcome prediction [5, 7–13]. Commonly employed algorithms include k-nearest neighbours (k-NN), support vector machines (SVM), decision trees (DT), logistic regression (LR), and random forest (RF), each of which has shown success in EEG-based biomedical classification tasks [6–13].

1.1. Literature review

Agarwal and Singhal [14] proposed a real-time schizophrenia (SZ) detection framework evaluated on the Warsaw dataset (14 SZ and 14 healthy controls [HC]). EEG signals were decomposed into sub-band components via the fast Fourier transform (FFT), from which statistical features were extracted alongside a novel look-ahead pattern (LAP) feature designed to capture local signal variations. Following Kruskal–Wallis feature selection, a boosted trees classifier achieved an accuracy of 98.62%, demonstrating the effectiveness of feature fusion strategies for EEG-based SZ detection.

Khare and Bajaj [15] proposed an adaptive decomposition framework for SZ detection using the Kaggle dataset (49 SZ and 32 HC). A flexible tunable Q wavelet transform (F-TQWT) optimized via grey wolf optimization (GWO) was employed for signal decomposition, followed by Kruskal–Wallis feature selection and a flexible least squares support vector machine (F-LSSVM) classifier. The model achieved 91.39% accuracy under ten-fold cross-validation.

Aydemir et al. [16] introduced CGP17Pat, a hand-crafted feature extraction method based on cyclic groups of prime order patterns, applied to the Warsaw dataset. Features were selected using iterative neighborhood component analysis (INCA) and classified with k-nearest neighbors (k-NN). A critical finding was the substantial gap between ten-fold cross-validation accuracy (99.91%) and leave-one-

subject-out (LOSO) accuracy (84.33%), highlighting the optimistic bias introduced by segment-level validation in small datasets.

Al-Azzawi and Uçan [17] investigated the impact of electrode reduction on SZ classification performance using the Warsaw dataset. Rather than utilizing all 19 channels, they compared random selection of 5 and 8 electrodes against principal component analysis (PCA)-based dimensionality reduction. Features were extracted via FFT and entropy measures (approximate entropy, log entropy, and Shannon entropy) and classified using k-NN, SVM, and quadratic discriminant analysis (QDA). The five-electrode configuration yielded competitive results, suggesting that clinically practical, reduced-channel EEG systems may be sufficient for automated SZ detection.

Ruiz de Miras et al. [12] evaluated a machine learning pipeline for SZ classification using resting-state EEG recordings from 11 SZ patients and 20 healthy controls. Linear and nonlinear measures were computed on sliding windows, followed by feature selection and dimensionality reduction via PCA. Five classifiers were then evaluated—k-NN, logistic regression (LR), decision tree (DT), random forest (RF), and SVM—with SVM achieving the highest AUC of 0.89.

Dhongade et al. [18] proposed a hybrid computer-aided detection system combining discrete wavelet transform (DWT) with a multilayer perceptron (MLP) neural network for SZ classification. DWT with a Daubechies (db4) wavelet at seven-level decomposition was used for sub-band feature extraction, validated on two public datasets: the Kaggle dataset and the Warsaw dataset. The proposed model achieved 99.61% and 99.12% accuracy on the two datasets, respectively, outperforming several prior methods. However, the absence of subject-independent validation such as LOSO raises concerns regarding the generalizability of the reported results.

1.2. Gap statement

Despite the promising results reported in prior studies, several critical limitations remain unresolved. First, many existing SZ detection frameworks have been validated on small-sample datasets (e.g., 14–49 SZ subjects), raising concerns about statistical power and generalizability. Second, the majority of studies rely on segment-level cross-validation, which has been shown to produce overly optimistic accuracy estimates—as high as 99.91%—compared to subject-level validation (e.g., leave-one-subject-out), which yields substantially lower performance. Third, prior work has predominantly employed hand-crafted features from a single domain (e.g., only frequency or only wavelet-based features), limiting the comprehensiveness of signal characterization. Fourth, while feature selection methods such as Kruskal–Wallis and neighborhood component analysis have been used, the application of recursive feature elimination—a powerful wrapper-based selection technique—remains underexplored for EEG-based SZ detection. Finally, few studies have systematically compared multiple machine learning classifiers on a unified, large-scale EEG database collected under controlled conditions.

1.3. Contribution of the study

To address the aforementioned gaps, this study introduces a new, larger EEG database comprising 51 SZ subjects and 50 HC—substantially exceeding the sample sizes of prior publicly available datasets. A comprehensive feature extraction strategy was employed, encompassing time-domain, frequency-domain, time–frequency, and nonlinear entropy-based features to capture diverse pathological signatures of SZ. To identify the most discriminative feature subset, Sequential Forward Selection (SFS) was applied, offering a systematic wrapper-based approach that iteratively removes redundant or irrelevant features. Subsequently, multiple machine learning classifiers—including but not limited to [insert e.g., SVM, random forest, k-NN, etc.]—were trained and evaluated under rigorous subject-wise cross-validation to ensure generalizability. The proposed framework provides a systematic comparison of classifier performance on a homogeneous, large-scale dataset, thereby offering a more reliable benchmark for automated SZ detection from EEG signals

2. Result

Table 1 summarizes the distribution of the 20 features selected by the Sequential Forward Selection (SFS) algorithm. Frequency-domain features constituted the majority of the selected subset (60.0%), with gamma-band features being the most frequently represented (20.0%), followed by alpha-band (15.0%), beta-band (10.0%), theta-band (10.0%), and delta-band (5.0%) features. Nonlinear features accounted for 25.0% of the selected subset, including permutation entropy, Higuchi fractal dimension, detrended fluctuation analysis, and Fisher information, highlighting the importance of signal complexity in schizophrenia discrimination. Time-domain and frequency-domain statistical features each contributed 5.0%, represented by the positive-to-negative peak ratio (PN_PkRatio) and median frequency, respectively. Overall, the SFS-selected subset demonstrates that combining spectral, nonlinear, and waveform-based EEG descriptors provides complementary information for distinguishing patients with schizophrenia from healthy controls.

Table 1
Distribution of the SFS-selected 20 EEG features across feature domains and sub-domains. Frequency-domain features constituted the largest proportion of the optimal feature subset, followed by nonlinear, time-domain, and frequency-domain statistical features.

Category	Sub-category	Count	%
Frequency-domain	Gamma band	4	20.0
	Alpha band	3	15.0
	Beta band	2	10.0
	Theta band	2	10.0
	Delta band	1	5.0
	Subtotal	**12**	**60.0**
Nonlinear	PermEn, HigFd, DetFluc, FishInfo	5	25.0
Time-domain	PN_PkRatio[1]	1	5.0
Frequency-domain statistical	Freq_Median	1	5.0
Total		**20**	**100.0**

[1] PN_PkRatio = |maximum positive peak| / |maximum negative peak|,

To comprehensively evaluate the discriminative capability of the selected EEG features, ten supervised machine learning classifiers were trained and tested using the LOSO CV protocol. This validation strategy ensures that data from each subject are used exclusively for testing once, providing an unbiased estimate of the models' generalization performance across individuals. Each classifier was trained separately using the optimal 20-feature subset selected by the Sequential Forward Selection (SFS-20) algorithm under both the EC and EO conditions. Tables 2 and 3 summarize the classification performance obtained for the EC and EO datasets, respectively. Under the EC condition (Table 2), Random Forest and XGBoost achieved the highest classification accuracy (81.44%), with Random Forest producing the best overall discrimination (AUC = 0.877), followed by AdaBoost (AUC = 0.865) and XGBoost (AUC = 0.864). In the EO condition (Table 3), XGBoost achieved the highest classification accuracy (78.35%), while MLP (Large) produced the highest AUC (0.853), closely followed by XGBoost (0.846) and Gradient Boosting (0.836). Overall, the EC condition consistently yielded higher classification performance than the EO condition, and the results indicate that tree-based ensemble methods generally outperformed conventional linear classifiers, suggesting that the discriminative information captured by the selected EEG features is better modeled through nonlinear decision boundaries.

Table 2
Classification performance of ten machine learning classifiers using the SFS-selected 20-feature subset under the EC condition with LOSO CV.

Classifier	Accuracy (%)	Specificity (%)	Sensitivity (%)	AUC
Random Forest	**81.44**	**86.00**	**76.60**	**0.877**
XGBoost	81.44	88.00	74.47	0.864
AdaBoost	79.38	84.00	74.47	0.865
Gradient Boosting	78.35	86.00	70.21	0.857
Decision Tree	76.29	80.00	72.34	0.847
Extra Trees	75.26	74.00	76.60	0.821
MLP (Large)	80.41	84.00	76.60	0.860
KNN (k = 5)	79.38	84.00	74.47	0.834
LDA	74.23	78.00	70.21	0.786
Logistic Regression	71.13	74.00	68.09	0.805

Table 3
Classification performance of ten machine learning classifiers using the SFS-selected 20-feature subset under the EO condition with LOSO CV.

Classifier	Accuracy (%)	Specificity (%)	Sensitivity (%)	AUC
Random Forest	75.26	80.00	70.21	0.825
XGBoost	**78.35**	**86.00**	**70.21**	**0.846**
AdaBoost	71.13	80.00	61.70	0.763
Gradient Boosting	76.29	86.00	65.96	0.836
Decision Tree	76.29	82.00	70.21	0.835
Extra Trees	64.95	94.00	34.04	0.774
MLP (Large)	76.29	86.00	65.96	0.853
KNN (k = 5)	71.13	90.00	51.06	0.795
LDA	57.73	72.00	42.55	0.721
Logistic Regression	70.10	76.00	63.83	0.809

2.1. SHAP-based feature importance analysis

To elucidate the decision-making process of the Random Forest classifier, SHAP analysis was conducted across all LOSO folds under the EC condition. Figure 1(a) presents the beeswarm summary

plot of the top 20 most influential features, where each point represents a single EEG segment; the color encodes the feature value (red = high, blue = low), and the horizontal position reflects its SHAP value, i.e., its contribution toward schizophrenia (SZ; positive SHAP values) or healthy control (HC; negative SHAP values). Figure 1(b) shows the corresponding mean absolute SHAP values, confirming the global importance ranking.

Among the top-ranked features, permutation entropy at channel 4 (PermEn_ch4) emerged as the most influential discriminative feature, followed by alpha-band power at channel 11 (alpha_Power_ch11), Higuchi fractal dimension at channel 7 (HigFd_ch7), and median frequency at channel 7 (Freq_Median_ch7). Other highly ranked features included the Positive-to-negative peak ratio (PN_Ratio_ch10), gamma-band mean power (gamma_Mean_ch7), delta-band median frequency (delta_Median_ch13), theta-band median frequency (theta_Median_ch17), detrended fluctuation analysis (DetFluc_ch7), and several additional spectral power and Fisher information measures. Overall, the SHAP ranking suggests that both nonlinear complexity measures and spectral EEG characteristics contributed substantially to the discrimination between SZ and HC, indicating that the Random Forest classifier relied on complementary information from multiple feature domains rather than a single dominant biomarker.

The box plot in Fig. 2(a) illustrates the monotonic relationship between PermEn_ch4 value groups (low, mid, and high tertiles) and their corresponding SHAP values. Segments with low permutation entropy exhibited strongly negative SHAP values, driving the classifier toward the HC class, whereas segments with high permutation entropy produced positive SHAP values, favoring SZ classification. The dependency plot in Fig. 2(b) further demonstrates an approximately linear relationship between PermEn_ch4 values and their SHAP contributions, indicating that increasing permutation entropy consistently increased the contribution of this feature toward SZ classification.

3. Discussion

This study developed a machine learning framework for SZ detection using resting-state EEG signals from the ASEEG dataset. Compared with existing public EEG datasets, ASEEG includes a relatively large cohort of participants, enabling a more reliable evaluation of machine learning models under LOSO cross-validation. Beyond classifier performance, the findings provide insights into the neurophysiological characteristics of SZ through explainable artificial intelligence. The discussion is organized around three principal findings: (1) the effectiveness of SFS combined with ensemble learning methods; (2) the diagnostic advantage of the EC condition over the EO condition; and (3) the complementary roles of spectral and nonlinear EEG features as biomarkers of SZ.

The best classification performance under the EC condition was achieved by Random Forest and XGBoost, each obtaining an accuracy of 81.44%, while Random Forest achieved the highest overall discriminative ability (AUC = 0.877). Under the EO condition, XGBoost achieved the highest accuracy (78.35%), whereas MLP produced the highest AUC (0.853). These findings demonstrate that ensemble

learning methods consistently outperformed conventional linear classifiers across both recording conditions.

The strong performance of ensemble models highlights the effectiveness of SFS. Unlike RFE, which removes features iteratively from a large feature set, SFS progressively constructs the optimal subset by adding the feature that provides the greatest improvement in classification performance at each iteration. This forward-search strategy efficiently reduces feature redundancy while preserving complementary information among EEG descriptors. By selecting only 20 highly informative features, SFS substantially reduced feature dimensionality while maintaining robust classification performance, thereby improving model interpretability and computational efficiency.

The superiority of Random Forest and other tree-based ensemble methods further suggests that the discriminative information contained in EEG signals is characterized by nonlinear relationships among multiple feature domains. Unlike linear classifiers, ensemble models effectively capture interactions between heterogeneous EEG descriptors, enabling more accurate representation of the complex neurophysiological alterations associated with SZ.

The classification performance achieved in this study is supported not only by the machine learning methodology but also by the quality of the ASEEG dataset. Compared with many publicly available SZ EEG datasets containing fewer than 50 participants, ASEEG provides recordings from 101 demographically matched subjects, improving statistical reliability and reducing the risk of model overfitting. In addition, standardized acquisition protocols and high-resolution EEG recordings provide a valuable resource for developing reproducible EEG biomarkers of SZ.

A distinctive characteristic of ASEEG is the inclusion of both EC and EO resting-state recordings. Across all evaluated classifiers, the EC condition consistently produced higher classification performance than the EO condition. This finding agrees with previous studies suggesting that intrinsic resting-state brain activity measured during EC recordings provides more stable neurophysiological signatures of SZ. Nevertheless, including both recording conditions expands the applicability of the dataset by enabling direct comparisons of biomarkers across different resting-state conditions and facilitating future multimodal investigations.

Analysis of the SFS-selected features revealed that frequency-domain features constituted the largest proportion of the optimal subset (60%), with gamma, alpha, beta, theta, and delta band features collectively dominating the selected feature set (Table 1). This predominance of spectral features is consistent with a growing body of literature reporting widespread abnormalities in resting-state EEG oscillations in SZ. Specifically, elevated resting-state gamma activity has been reported as a consistent neurophysiological signature of SZ, attributed to dysfunction of parvalbumin-containing interneurons and disrupted excitatory-inhibitory balance [31]. Similarly, alterations in alpha-band oscillations have been documented across multiple resting-state EEG studies, with abnormal alpha activity proposed as a diagnostic biomarker for SZ [32].

Although spectral features represented the majority of the selected subset, SHAP analysis demonstrated that feature frequency did not necessarily correspond to discriminative importance. The most influential feature was permutation entropy at the frontal midline electrode Fz (PermEn_ch4), followed by alpha-band power at the right temporal region (T4), Higuchi fractal dimension, median frequency, and gamma-band mean power at the left temporal region (T3). This apparent discrepancy is neurophysiologically plausible: spectral features provide broad coverage of oscillatory abnormalities across multiple frequency bands, whereas nonlinear complexity measures capture alterations in signal regularity and information processing that are highly characteristic of SZ [33]. Consequently, these two feature domains should be regarded as complementary rather than competing biomarkers.

Anatomically, the highest-ranking SHAP features were primarily distributed across the frontal (Fz), temporal (T3 and T4), and central (C4) regions. The prominence of PermEn at the frontal midline supports previous evidence implicating frontal dysfunction in SZ, whereas the importance of temporal spectral and nonlinear features is consistent with reports of disrupted fronto-temporal networks involved in cognitive processing and sensory integration [34–39]. Together, these findings suggest that SZ is characterized not by abnormalities within a single EEG domain, but by complementary alterations in neural oscillations, signal complexity, and waveform morphology distributed across multiple brain regions.

In summary, this study demonstrates that SFS, combined with ensemble learning and SHAP, effectively identified a compact and informative EEG feature subset for SZ classification. The consistently superior performance obtained under the EC condition further supports the hypothesis that intrinsic resting-state brain activity provides more discriminative biomarkers than the EO condition. Future work should validate these findings using independent datasets and investigate advanced deep learning approaches while preserving model interpretability.

To place the performance of the proposed framework into context, we compared our results with previous EEG-based SZ classification studies that primarily used the publicly available Warsaw dataset (Table 3). Unlike ASEEG, which contains recordings from 101 participants (51 SZ and 50 HC), the Warsaw dataset comprises only 28 participants (14 SZ and 14 HC). Such limited sample sizes often increase the risk of optimistic performance estimates and reduce the generalizability of reported models.

As shown in Table 3, several studies reported classification accuracies exceeding 95%. However, most of these investigations employed 10-fold cross-validation, in which EEG segments from the same subject may appear in both training and testing folds. Consequently, these validation strategies can produce overly optimistic estimates by exploiting subject-specific characteristics rather than disease-related biomarkers. In contrast, the present study employed the more stringent LOSO protocol, ensuring complete subject independence between training and testing data and providing a more realistic estimate of model generalization.

Although the proposed framework achieved a lower classification accuracy (81.44%) than some previous reports, the evaluation protocol is substantially more rigorous and was performed on a considerably larger cohort. Therefore, the obtained performance is likely to better reflect real-world clinical applicability. Furthermore, the integration of SFS, ensemble learning, and SHAP provides not only competitive diagnostic performance but also improved interpretability by identifying biologically meaningful EEG biomarkers associated with SZ.

Table 3
Comparative Analysis of Existing Benchmarks

Ref	Dataset (SZ/ HC)	Split	Method	Accuracy (%)	Sensitivity (%)	Specificity (%)	AUC
Li et al., [40]	Warsaw (14/14)	LOSO	Microstate semantic modeling; dual templates	96.40	96.20	96.50	-
Prabhakar et al., [41]	Warsaw (14/14)	70% train, 30% test	Nonlinear features, Swarm Intelligence Computing Techniques, SVM, KNN, QDA, ANN, FLDA, LR	89.85	-	-	-
Baygin [42]	Warsaw (14/14)	10-fold CV	TQWT sub-bands coefficients, ReliefF, Ensemble Subspace KNN	99.12	-	-	1.00
Kim et al., [43]	Warsaw (14/14)	10-fold CV	Microstate features, conventional features (time, frequency, statistical), RFE, SVM	75.64	71.93	75.50	0.80
Gosala et al., [44]	Warsaw (14/14)	10-fold CV	DWT, CWT, SVM, KNN, LR, DT, adaboost, GB	97.98	98.20	97.72	-
Akbari et al.,[45]	Warsaw (14/14)	10-fold CV	Phase Space Dynamic, graphical Features, KNN	94.80	94.30%	95.20%	-
Aydemir et al., [16]	Warsaw (14/14)	10-fold CV & LOSO	cyclic group of prime order pattern, INCA, KNN, majority voting	99.91 (10-fold CV), 84.33 (LOSO)	99.84 (10-fold CV), 77% (LOSO)	100 (10-fold CV), 93.22 (LOSO)	-
Chien et al., [46]	Warsaw (14/14)	10-fold CV	Frequency rhythms, Sequential minimal	92%	-	-	-

Ref	Dataset (SZ/HC)	Split	Method	Accuracy (%)	Sensitivity (%)	Specificity (%)	AUC
			optimization, RF				
Ours	Our (51/50)	LOSO	SFS-20 + Random Forest (EC)	81.44	76.60	86.00	0.877

Key contributions of this study include:

1- The combination of SFS and LOSO produced an interpretable and computationally efficient framework while minimizing the risk of data leakage.

2- Random Forest and XGBoost consistently achieved the best performance under the EC condition, indicating that nonlinear ensemble models effectively capture the complex interactions among EEG features.

3- SHAP analysis identified PermEn at Fz as the most influential feature, followed by alpha-band power at T4, and Higuchi fractal dimension, median frequency, and gamma-band mean power at T3, highlighting complementary contributions from frontal, temporal, and central brain regions.

4- The consistently better performance obtained under the EC condition supports previous evidence that intrinsic resting-state brain activity provides more discriminative biomarkers than recordings acquired during the EO condition.

Despite the relatively large cohort compared with many previous EEG studies, the ASEEG dataset was collected at a single clinical center. Consequently, although the proposed framework demonstrated robust performance under LOSO validation, additional evaluation on independent multi-center datasets is required to establish its generalizability across different recording protocols and patient populations.

Another limitation is that only handcrafted EEG features were investigated. Although SFS successfully identified a compact and informative subset of features, future studies should explore hybrid approaches that combine handcrafted biomarkers with deep learning representations. In addition, while SHAP identified the most influential EEG biomarkers, future work should investigate their relationships with clinical symptoms, disease severity, and treatment response to further enhance their clinical relevance.

4. Conclusion

This study demonstrated the feasibility of combining SFS, ensemble machine learning, and SHAP explainability for EEG-based SZ classification using the ASEEG dataset, which comprises 101 demographically matched participants (51 SZ and 50 HC). Compared with many previous studies that

relied on smaller public datasets, the larger cohort and LOSO evaluation protocol provide a more rigorous assessment of model generalization. Among the evaluated classifiers, Random Forest and XGBoost achieved the highest classification accuracy (81.44%) under the EC condition, with Random Forest providing the best overall discrimination (AUC = 0.877). Under the EO condition, XGBoost achieved the highest accuracy (78.35%), whereas MLP yielded the highest AUC (0.853). SHAP analysis further demonstrated that PermEn at Fz was the most influential biomarker, followed by alpha-band power at T4, and Higuchi fractal dimension, median frequency, and gamma-band mean power at T3. These findings indicate that complementary spectral and nonlinear EEG features distributed across frontal, temporal, and central regions contribute to SZ discrimination. Overall, the proposed framework provides an interpretable and robust approach for automated SZ detection and establishes a strong foundation for future validation on independent multi-center EEG datasets.

5. Material and Method

5.1. Participants and recording

In this study we have processed the ASEEG dataset [19, 20]. This dataset includes EEG recordings from 51 patients diagnosed with SZ (average age: 31.29 ± 13.63 years; age range: 15–65 years; 15 females, representing 29.41%) alongside 50 healthy volunteers free of neurological or psychiatric conditions (average age: 29.4 ± 8.3 years; age range: 18–52 years; 33 females, representing 66%). Table 4 reports demographic information about this database.

Table 4
Demographic details from participants

Group	Number (female/male)	Age (female/male)	Criteria	Channels (sampling rate, Hz)
SZ	51 (15/36)	31.29 ± 13.63	DSM-5	19 (500)
Normal	50 (33/17)	29.40 ± 8.30	-	

EEG signals were obtained retrospectively from the clinic's medical records. All recordings took place in a controlled clinical environment, conducted by a qualified technician with a 21-channel Mitsar EEG device (Mitsar Co. Ltd., Russia). Nineteen scalp electrodes followed the standard 10–20 system were recorder. Data were captured at a sampling rate of 500 Hz, with A1 and A2 electrodes positioned on the ears to serve as reference and ground leads, respectively. Protocols focused on resting-state conditions involving both eyes-open (EO) and eyes-close (EC) segments, while sleep-stage recordings were omitted to minimize potential influences from varying arousal levels.

ASEEG data recording condition was approved by the Ethics Review Board of Shahid Beheshti University of Medical Sciences under ethics approval number IR.SBMU.MSP.REC.1404.441 and was conducted in accordance with the Declaration of Helsinki and local ethical regulations. Written informed consent was obtained from all participants or their legal guardians before EEG recording and data collection. For

participants under 18 years of age or those unable to provide independent consent, written authorization was obtained from a parent or legal guardian. All data were de-identified to protect participant privacy, and participants were informed of their right to withdraw from the study at any time without consequence.

Diagnoses of SZ were confirmed separately by two experienced psychiatrists using DSM-5 guidelines. HCs consisted of individuals undergoing standard EEG evaluations for reasons not linked to mental health or neurological issues. Exclusion criteria for controls encompassed prior diagnoses of bipolar disorder, substance use disorders, any psychiatric or somatic illnesses necessitating inpatient care, seizures or antiseizure medication use, history of electroconvulsive treatment, vagus nerve stimulation, or repetitive transcranial magnetic stimulation. Further disqualifiers involved head trauma or radiological findings suggestive of vascular brain pathology (either ischemic or hemorrhagic types). Figure 3 shows 19-EEG signals in (a) and (c) SZ subject and (b) and (d) HC subject during eyes open and close conditions, respectively.

5.2. EEG Preprocessing

Preprocessing was performed in MATLAB R2025a using EEGLAB. Continuous data were band-passed filtered between 1 and 45 Hz with 4th order Butterworth-characteristic filters to suppress slow drifts and high-frequency noise before downstream analysis. Then, signals were downsampled to 128 Hz due to simple processing and reduce computational costs. After that, signals were divided into non-overlapping 30 second segments to generate images from them.

5.3. Feature Extraction

To comprehensively analyze the EEG signals for potential schizophrenic biomarkers, a rich set of features was extracted directly from the raw signal data. This approach minimizes preprocessing and captures information from distinct signal domains (time, frequency, and nonlinear) to provide a holistic description of the signal dynamics.

5.3.1. Time-Domain Features

Time-domain features describe the statistical and morphological characteristics of the signal waveform. This category includes fundamental statistical moments such as the mean, median, standard deviation (Std), and variance (Var) of the signal amplitude, along with the maximum (Max) and minimum (Min) values. Higher-order statistics were also computed, including skewness (Skew), to assess the asymmetry of the amplitude distribution, and kurtosis (Kur), to measure its "tailedness." Further morphological descriptors included the zero-crossing rate (zCross), which quantifies the number of times the signal polarity changes, and peak-based features to further characterize the signal’s dynamic fluctuations [21].

5.3.2. Frequency-Domain Features

To analyze the spectral content, the Power Spectral Density (PSD) of the signal was first estimated using Welch's method [21]. This technique provides a robust spectrum estimation by averaging the periodograms of overlapping, windowed signal segments. From the PSD, statistical features (mean, std, skew, kurtosis) were computed across the entire spectrum. Crucially, the relative band power was calculated for the five standard EEG frequency bands: Delta (1–4 Hz), Theta (4–8 Hz), Alpha (8–13 Hz), Beta (13–25 Hz), and Gamma (25–45 Hz). These features represent the distribution of signal energy across different neural rhythms. Spectral Entropy was also computed as a measure of the PSD's complexity and flatness.

5.3.3. Nonlinear Features

Entropy features quantify the regularity, predictability, and complexity of the time series. Several entropy measures were computed: Approximate Entropy (ApEn) and Sample Entropy (SampEn) are robust measures of regularity that are particularly effective for analyzing noisy, real-world biological signals [22, 23]. Permutation Entropy (PermEn) assesses complexity based on ordinal patterns (the rank order of values) within the signal, offering a computationally efficient and robust alternative to other entropy measures. Shannon Entropy (ShanEn) was also used to measure the overall uncertainty in the signal's amplitude distribution.

This category of features quantifies the non-linear, chaotic, and fractal dynamics of the EEG signal. Hjorth parameters, specifically Mobility (representing the mean frequency) and Complexity (representing the change in frequency), were calculated. Lempel-Ziv Complexity (LZC) was employed to measure the rate of new pattern emergence in the binarized time series, reflecting its algorithmic complexity [22]. Furthermore, several Fractal Dimension (FD) metrics, including Petrosian FD, Katz FD, and Higuchi FD, were computed to assess the self-similarity and geometric complexity of the signal waveform [24].

5.4. Optimum Feature Selection using SFS method

The comprehensive extraction process resulted in a high-dimensional feature space. Such high dimensionality can lead to the curse of dimensionality, increased computational cost, and model overfitting. Therefore, a critical step was to apply a feature selection technique that identifies a small, highly discriminative subset of features while eliminating redundant and irrelevant variables. SFS is a classical wrapper-based feature selection technique [25]. Unlike backward-elimination approaches, SFS builds the feature subset incrementally: starting from an empty set, it repeatedly adds the single feature whose inclusion yields the greatest improvement in cross-validated model performance, until a pre-specified target subset size is reached.

The SFS process applied in this study proceeded as follows:

1. Starting from an empty feature subset S = {}, each remaining candidate feature was temporarily added to S and the resulting subset was evaluated via cross-validated classification performance.
2. The candidate feature that produced the greatest improvement in the evaluation criterion was permanently added to S.

3. Steps 1–2 were repeated, with each iteration adding one feature to S, until the target subset size of $k = 20$ features was reached, separately for the EC and EO conditions.
4. The resulting 20-feature subsets - ranked by selection order - are reported in Table 1.

5.5. Machine Learning Classification

Following the feature-selection phase—where optimal subsets were identified using SFS—the refined feature sets were utilized to train and evaluate a comprehensive set of twenty machine-learning classifiers. The objective was to identify the most robust and generalizable model for SZ classification through comparative evaluation across diverse algorithmic families.

These classifiers represented a wide range of learning paradigms, including instance-based (k-NN), kernel-based (SVM with Linear, RBF, and Polynomial kernels) [26], neural (MLP), ensemble (Bagging and Boosting methods like Random Forest and XGBoost [27, 28], linear (Logistic Regression, LDA), probabilistic models and a single estimator baseline (Decision Tree with max_depth = 10) [29]. Each classifier was trained and validated using a LOSO cross-validation framework to ensure subject-level independence and robustly assess generalization capability. All models were implemented using standard configurations, with specific hyperparameter tuning (e.g., varying network depths for MLPs, different k for k-NN) applied to optimize performance across the various algorithmic types.

5.6. Model Explainability (SHAP Analysis)

To enhance the interpretability of the proposed classification framework, SHapley Additive exPlanations (SHAP) were applied to the best-performing classifier, Random Forest, following LOSO cross-validation [30]. SHAP values were computed using the TreeExplainer, with feature contributions aggregated across all LOSO folds to provide a subject-independent measure of feature importance. This approach quantifies the contribution of each feature to the model's predictions, enabling both global (population-level) and local (sample-level) interpretability while identifying the EEG biomarkers that most strongly influenced schizophrenia classification.

5.7. Evaluation Protocol

Each classifier was evaluated under the LOSO CV scheme, ensuring that no subject’s data contributed to both training and testing phases. Performance was quantified using multiple standard metrics, including Accuracy, Precision, Recall, F1-Score, and Area Under the ROC Curve (AUC). This multi-metric assessment provided a comprehensive evaluation of classifier behavior across various performance dimensions [13].

5.8. Overview of the study

The overall workflow of the proposed EEG-based schizophrenia classification framework is illustrated in Fig. 4. The pipeline begins with the acquisition of raw EEG recordings, followed by a series of preprocessing steps to improve signal quality and remove unwanted artifacts. A diverse set of features is then extracted to capture temporal, spectral and nonlinear characteristics of brain activity. To ensure

robust subject-independent evaluation, a LOSO CV strategy is employed. Subsequently, SFS is used to identify the most discriminative features, which are then provided to multiple classical machine learning classifiers. To enhance the interpretability of the developed models, SHAP is applied to quantify the contribution of individual features to the classification outcome. The final stage of the framework aims to accurately distinguish patients with schizophrenia from healthy control subjects.

Declarations

Ethics approval and consent to participate

In this study we used available ASEEG database [19,20]. Recording was approved by the Ethics Review Board of Shahid Beheshti University of Medical Sciences under ethics approval number IR.SBMU.MSP.REC.1404.441 and was conducted in accordance with the Declaration of Helsinki and local ethical regulations. Written informed consent was obtained from all participants or their legal guardians before EEG recording and data collection. For participants under 18 years of age or those unable to provide independent consent, written authorization was obtained from a parent or legal guardian. All data were de-identified to protect participant privacy, and participants were informed of their right to withdraw from the study at any time without consequence.

Consent for publication

Written informed consent was obtained from all participants or their legal guardians before EEG recording and data collection for publication.

Availability of data and materials

In this study we have used the public available ASEEG database [19,20]. You can download it from here: https://zenodo.org/uploads/18029536.

Competing interests

There are no competing interests.

Funding

There is no fund for this study.

Author contributions

M.R. N.: Conceptualization, Methodology, Investigation, Validation, Writing—original draft. F. F.: Conceptualization, Methodology, Software, Investigation, Validation, Writing—original draft, Writing—review & editing. A.H. Gh.: Conceptualization, Methodology, Software, Investigation, Validation. S. B.: Conceptualization, Methodology, Software, Investigation, Validation, Writing—original draft, Writing—

review & editing. P. T. K.: Conceptualization, Methodology, Investigation, Validation, Writing—original draft. A. Sh.: Conceptualization, Methodology, Validation, Supervision, Writing—review & editing.

Acknowledgement

Not applicable.

References

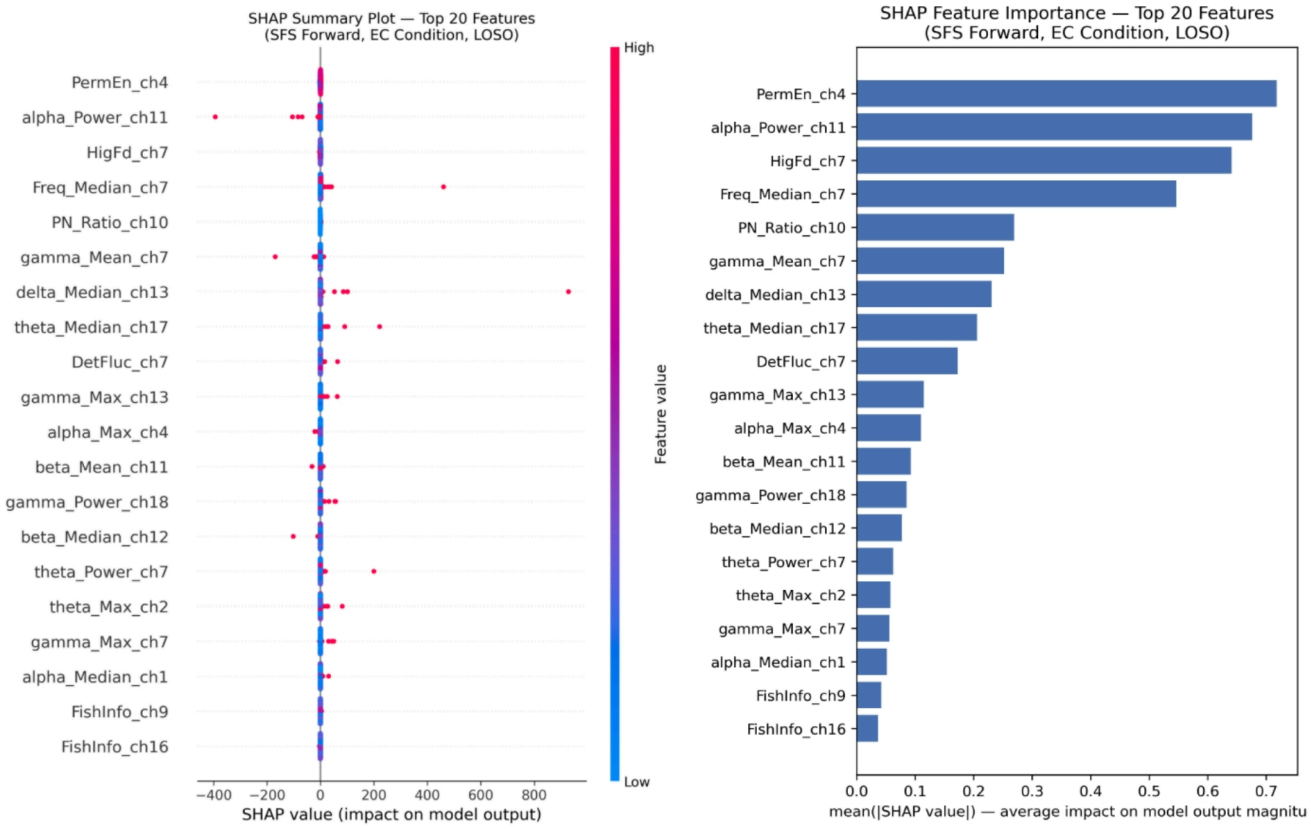
1. Solmi M, Seitidis G, Mavridis D, Correll CU, Dragioti E, Guimond S, Tuominen L, Dargél A, Carvalho AF, Fornaro M, Maes M. Incidence, prevalence, and global burden of schizophrenia-data, with critical appraisal, from the Global Burden of Disease (GBD) 2019. Molecular psychiatry. 2023;28(12):5319–27.
2. Mattila T, Koeter M, Wohlfarth T, Storosum J, van den Brink W, de Haan L, Derks E, Leufkens H, Denys D. Impact of DSM-5 changes on the diagnosis and acute treatment of schizophrenia. Schizophrenia bulletin. 2015;41(3):637–43.
3. International Statistical Classification of Diseases and Related Health Problems 10th Revision (ICD-10) Version for 2010 [Internet]. Geneva: World Health Organization; [cited 2026 Jun 20]. Available from: https://icd.who.int/browse10/2010/en#/F20-F29
4. Kim HK, Blumberger DM, Daskalakis ZJ. Neurophysiological biomarkers in schizophrenia—P50, mismatch negativity, and TMS-EMG and TMS-EEG. Frontiers in Psychiatry. 2020;11:795.
5. Yun S. Advances, challenges, and prospects of electroencephalography-based biomarkers for psychiatric disorders: a narrative review. Journal of Yeungnam Medical Science. 2024;41(4):261–8.
6. Shim M, Hwang HJ, Kim DW, Lee SH, Im CH. Machine-learning-based diagnosis of schizophrenia using combined sensor-level and source-level EEG features. Schizophrenia research. 2016;176(2–3):314–9.
7. Naeim M, Narimani M. EEG-based biomarkers for psychosis: Comparative performance of support vector machines and deep neural networks. Biological Psychology. 2026; 205: 109232
8. Hassan F, Hussain SF, Qaisar SM. Fusion of multivariate EEG signals for schizophrenia detection using CNN and machine learning techniques. Information Fusion. 2023; 92:466–78.
9. Sravanthi GS, Sharma LD. Schizophrenia detection via lobe-wise and overall EEG features using VMD and bayesian-optimized machine learning models. Front. Neurosci. 2026; 20:1753779. doi: 10.3389/fnins.2026.1753779
10. Al Mazroa A, Eltahir MM, Ebad SA, Alotaibi FA, Cho J. EEG-based schizophrenia diagnosis using deep learning with multi-scale and adaptive feature selection. PeerJ Computer Science. 2025;11:e2811.
11. Han X, Emara Y, Zhang A, Lin Y, Zhang Y. Configurable Modular EEG Classification Framework with Multiscale Features and Ensemble Learning: A Reproducible Evaluation for Schizophrenia Detection. Bioengineering. 2026;13(4):430.

12. J. Ruiz de Miras, A. J. Ibáñez-Molina, M. F. Soriano, and S. Iglesias-Parro, "Schizophrenia classification using machine learning on resting state EEG signal," Biomed. Signal Process. Control, vol. 79, p. 104233, Jan. 2023, doi: 10.1016/j.bspc.2022.104233.
13. J. Rahul, D. Sharma, L. D. Sharma, U. Nanda, and A. K. Sarkar, “A systematic review of EEG based automated schizophrenia classification through machine learning and deep learning,” 2024, *Frontiers Media SA*. doi: 10.3389/fnhum.2024.1347082.
14. M. Agarwal and A. Singhal, "Fusion of pattern-based and statistical features for schizophrenia detection from EEG signals," Med. Eng. Phys., vol. 112, p. 103949, Feb. 2023, doi: 10.1016/j.medengphy.2023.103949.
15. S. K. Khare and V. Bajaj, "A self-learned decomposition and classification model for schizophrenia diagnosis," Comput. Methods Programs Biomed., vol. 211, p. 106450, Nov. 2021, doi: 10.1016/j.cmpb.2021.106450.
16. E. Aydemir et al., "CGP17Pat: Automated schizophrenia detection based on a cyclic group of prime order patterns using EEG signals," Healthcare, vol. 10, no. 4, p. 643, Mar. 2022, doi: 10.3390/healthcare10040643.
17. A. Al-Azzawi and O. N. Uçan, "Investigate schizophrenia classification based on EEG electrode reduction using machine learning techniques," Traitement du Signal, vol. 42, no. 3, 2025, doi: 10.18280/ts.420340.
18. Dhongade D, Captain K, Dahiya S. EEG-based schizophrenia detection: Integrating discrete wavelet transform and deep learning. Cognitive Neurodynamics. 2025;19(1):62.
19. Bagherzadeh, S., Norouzi, M., Farokhshad, F., Tolou Koroushi, P., Ghasri, A., Bahri Hampa, S., Kazemi, R., Rostami, R., & Shalbaf, A. (2025). ASEEG: Atieh Schizophrenia EEG, a novel high-quality dataset designed to advance biomarker research (First version) [Data set]. Zenodo. https://doi.org/10.5281/zenodo.18029536
20. Bagherzadeh, S., Norouzi, M., Farokhshad, F., Tolou Koroushi, P., Ghasri, A., Kazemi, R., Rostami, R., & Shalbaf, A. (2026). Atieh Schizophrenia EEG, a novel high-quality dataset designed to advance biomarker and machine learning research, scientific data, 2026.
21. Bagherzadeh S, Maghooli K, Farhadi J, Zangeneh Soroush M. Emotion recognition from physiological signals using parallel stacked autoencoders. Neurophysiology. 2018;50(6):428–35. doi: 10.1007/s11062-019-09775-y.
22. Stancin I, Cifrek M, Jovic A. A review of EEG signal features and their application in driver drowsiness detection systems. Sensors. 2021;21(11):3786.
23. Ehtiati N, Attarodi G, Dabanloo NJ, Sedehi JF, Nasrabadi AM. Prediction of ventricular tachycardia using nonlinear features of heart rate variability signal such as poincare plot, approximate and sample entropy, recurrence plot. In 2017 Computing in Cardiology (CinC) 2017 Sep 24 (pp. 1–4). IEEE.
24. Bai Y, Liang Z, Li X. A permutation Lempel-Ziv complexity measure for EEG analysis. Biomedical Signal Processing and Control. 2015;19:102–14.

25. Marcano-Cedeño A, Quintanilla-Domínguez J, Cortina-Januchs MG, Andina D. Feature selection using sequential forward selection and classification applying artificial metaplasticity neural network. InIECON 2010-36th annual conference on IEEE industrial electronics society 2010 Nov 7 (pp. 2845–2850). IEEE.
26. I. Guyon, J. Weston, and S. Barnhill, “Gene Selection for Cancer Classification using Support Vector Machines,” 2002.
27. R. Polikar, “Ensemble based systems in decision making,” IEEE Circuits and Systems Magazine, vol. 6, no. 3, pp. 21–45, 2006, doi: 10.1109/MCAS.2006.1688199.
28. Sagi, Omer, and Lior Rokach. "Ensemble learning: A survey." Wiley interdisciplinary reviews: data mining and knowledge discovery 8, no. 4 (2018): e1249.
29. I. Mienye and N. Jere, “A Survey of Decision Trees: Concepts, Algorithms, and Applications,” IEEE Access, vol. PP, p. 1, Jan. 2024, doi: 10.1109/ACCESS.2024.3416838.
30. Mosca E, Szigeti F, Tragianni S, Gallagher D, Groh G. SHAP-based explanation methods: a review for NLP interpretability. InProceedings of the 29th international conference on computational linguistics 2022 Oct (pp. 4593–4603).
31. M. Sabeti, S. Katebi, and R. Boostani, “Entropy and complexity measures for EEG signal classification of schizophrenic and control participants,” Artif Intell Med, vol. 47, no. 3, pp. 263–274, 2009, doi: https://doi.org/10.1016/j.artmed.2009.03.003.
32. S. K. Tikka et al., “Artificial intelligence-based classification of schizophrenia: A high density electroencephalographic and support vector machine study,” Indian J Psychiatry, vol. 62, no. 3, pp. 273–282, May 2020, doi: 10.4103/psychiatry.IndianJPsychiatry_91_20.
33. Liu Y, Xu P, Hu S. Resting-state gamma power in schizophrenia: a systematic review and meta-analysis. Frontiers in Psychiatry. 2026;16:1731645.
34. Han C, Wang B, Peng X, Li M, Zhang Z, Yao C, Tu M, Chen X, Zhou J, Wang C, Zhao X. Distinct oscillatory mechanisms in low and high alpha-band activities for screening and potential treatment of Schizophrenia. Translational Psychiatry. 2025;15(1):210.
35. D. Bai, W. Yao, S. Wang, and J. Wang, “Multiscale Weighted Permutation Entropy Analysis of Schizophrenia Magnetoencephalograms,” Entropy, vol. 24, no. 3, Mar. 2022, doi: 10.3390/e24030314.
36. Ruiz de Miras J, Ibáñez-Molina AJ, Soriano MF, Iglesias-Parro S. Fractal dimension analysis of resting state functional networks in schizophrenia from EEG signals. Frontiers in Human Neuroscience. 2023;17:1236832.
37. John JP. Fronto-temporal dysfunction in schizophrenia: A selective review. Indian journal of psychiatry. 2009;51(3):180–90.
38. Bagherzadeh S, Shahabi MS, Shalbaf A. Detection of schizophrenia using hybrid of deep learning and brain effective connectivity image from electroencephalogram signal. Computers in Biology and Medicine. 2022;146:105570.

39. Bagherzadeh S, Shalbaf A. EEG-based schizophrenia detection using fusion of effective connectivity maps and convolutional neural networks with transfer learning. Cognitive Neurodynamics. 2024;18(5):2767–78.
40. H. Li, C. Wang, L. Ma, C. Xu, and H. Li, “EEG analysis in patients with schizophrenia based on microstate semantic modeling method,” *Front Hum Neurosci*, vol. 18, 2024, doi: 10.3389/fnhum.2024.1372985.
41. S. K. Prabhakar, H. Rajaguru, and S.-H. Kim, “Schizophrenia EEG Signal Classification Based on Swarm Intelligence Computing,” Comput Intell Neurosci, vol. 2020, pp. 1–14, Nov. 2020, doi: 10.1155/2020/8853835.
42. M. Baygin, “An accurate automated schizophrenia detection using TQWT and statistical moment based feature extraction,” Biomed Signal Process Control, vol. 68, p. 102777, Jul. 2021, doi: 10.1016/j.bspc.2021.102777.
43. K. Kim, N. T. Duc, M. Choi, and B. Lee, “EEG microstate features for schizophrenia classification,” PLoS One, vol. 16, no. 5, p. e0251842, May 2021, doi: 10.1371/journal.pone.0251842.
44. B. Gosala, P. Dindayal Kapgate, P. Jain, R. Nath Chaurasia, and M. Gupta, “Wavelet transforms for feature engineering in EEG data processing: An application on Schizophrenia,” Biomed Signal Process Control, vol. 85, p. 104811, Aug. 2023, doi: 10.1016/j.bspc.2023.104811.
45. H. Akbari, S. Ghofrani, P. Zakalvand, and M. Tariq Sadiq, “Schizophrenia recognition based on the phase space dynamic of EEG signals and graphical features,” Biomed Signal Process Control, vol. 69, Aug. 2021, doi: 10.1016/j.bspc.2021.102917.
46. F. Chien, V. L. Kouznetsova, S. Kesari, and I. F. Tsigelny, “Electroencephalography-based diagnosis of schizophrenia using machine learning,” Cerebral Cortex, vol. 35, no. 7, Jul. 2025, doi: 10.1093/cercor/bhaf184.

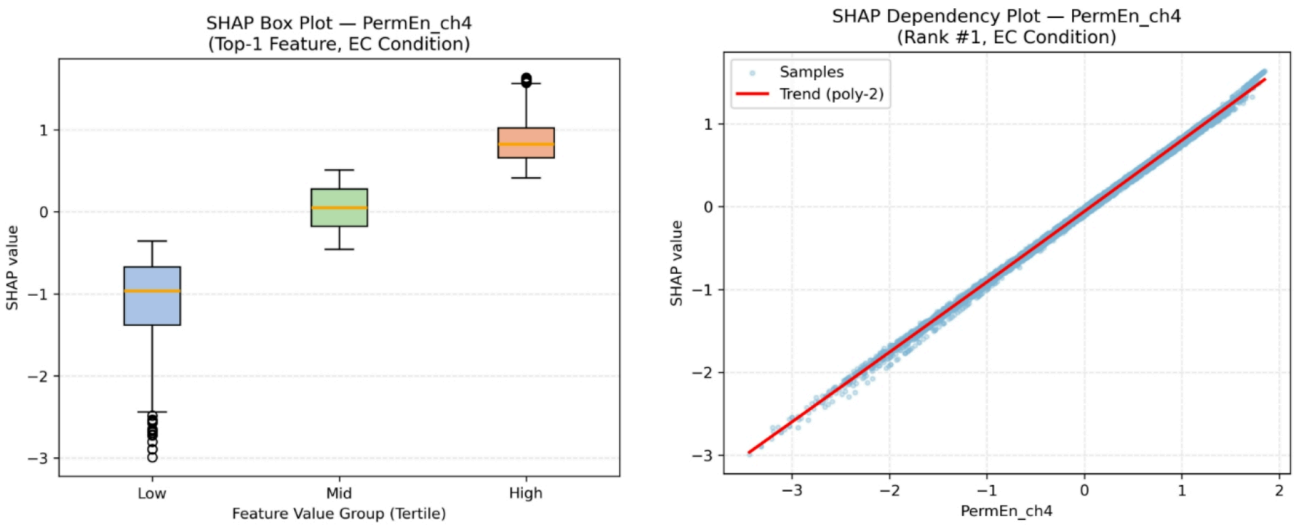
Figures



(a) (b)

Figure 1

SHAP-based global feature-importance analysis of the Random Forest classifier under the eyes-closed (EC) condition, aggregated across all LOSO folds. (a) Beeswarm summary plot of the top 20 SEF-selected features ranked by mean absolute SHAP value. Each point represents one EEG segment; color encodes the normalized feature value (red = high, blue = low), and horizontal position indicates the SHAP contribution, where positive values push the model toward SZ classification and negative values toward HC. PermEn_ch4 emerged as the most influential feature. (b) Bar chart of mean absolute SHAP values for the top 20 features, confirming the global importance ranking. The highest-ranked features included PermEn_ch4, alpha_Power_ch11, HigFd_ch7, and Freq_Median_ch7, demonstrating that the classifier exploited complementary information from nonlinear complexity measures, spectral power, and frequency-domain descriptors. Note: channels order are Fp1, Fp2, F7, F3, Fz, F4, F8, T3, C3, Cz, C4, T4, T5, P3, Pz, P4, T6, O1, O2.



(a) (b)

Figure 2

SHAP-based analysis of the relationship between PermEn_ch4 and its contribution to the Random Forest classifier under the eyes-closed (EC) condition, aggregated across all LOSO folds. (a) Box plot of SHAP values for PermEn_ch4 stratified by feature-value tertiles (low, mid, and high), illustrating a monotonic increase in SHAP contribution with increasing permutation entropy. (b) SHAP dependency plot for PermEn_ch4, demonstrating an approximately monotonic relationship between feature value and SHAP contribution, indicating that higher permutation entropy consistently increased the feature's contribution toward SZ classification.

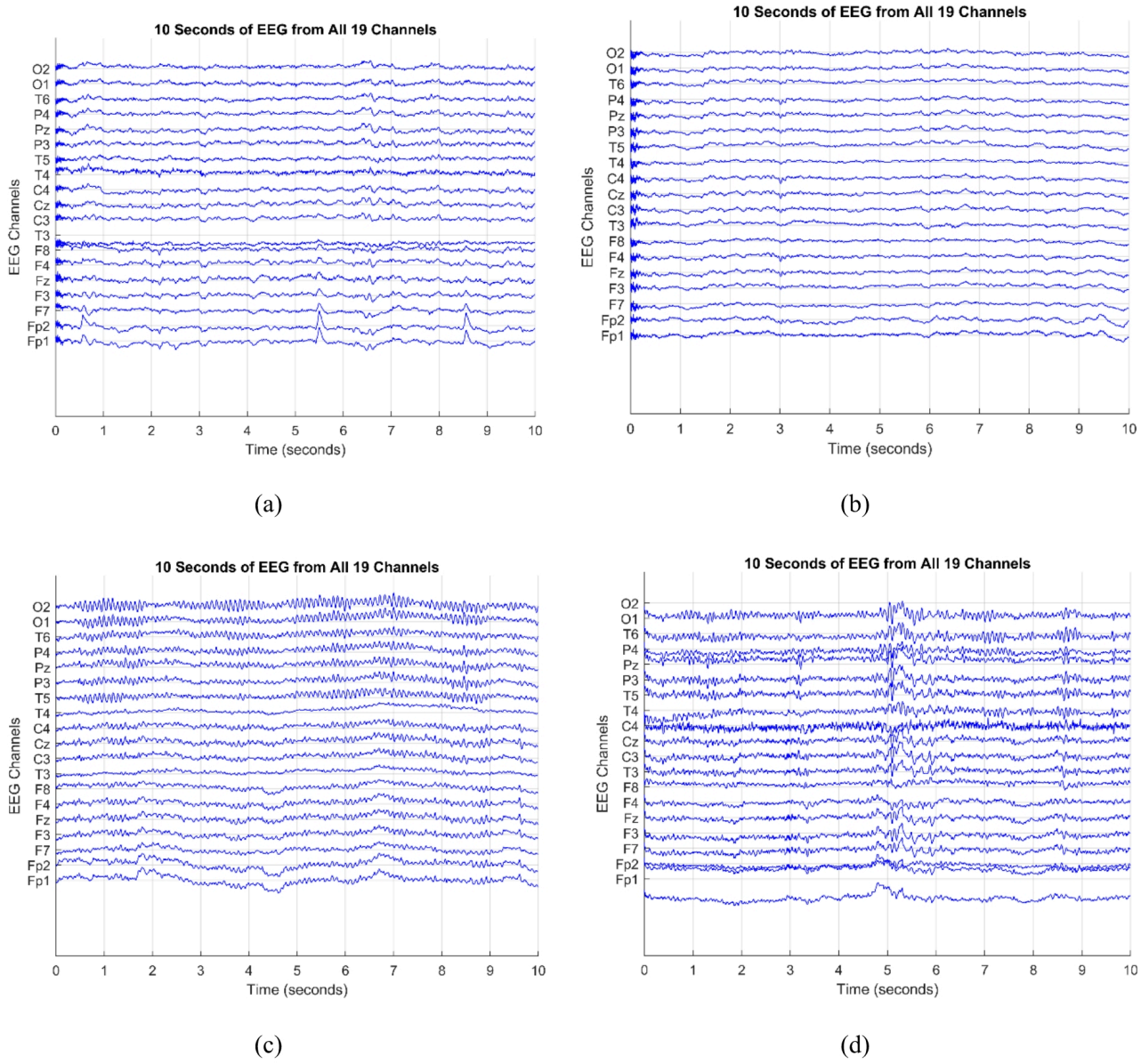


Figure 3

An example from 19 EEG channels of (a) and (c) SZ subject and (b) and (d) normal subject during eyes open and close conditions, respectively. Horizontal axis is time and vertical is amplitude of signal in micro volts.

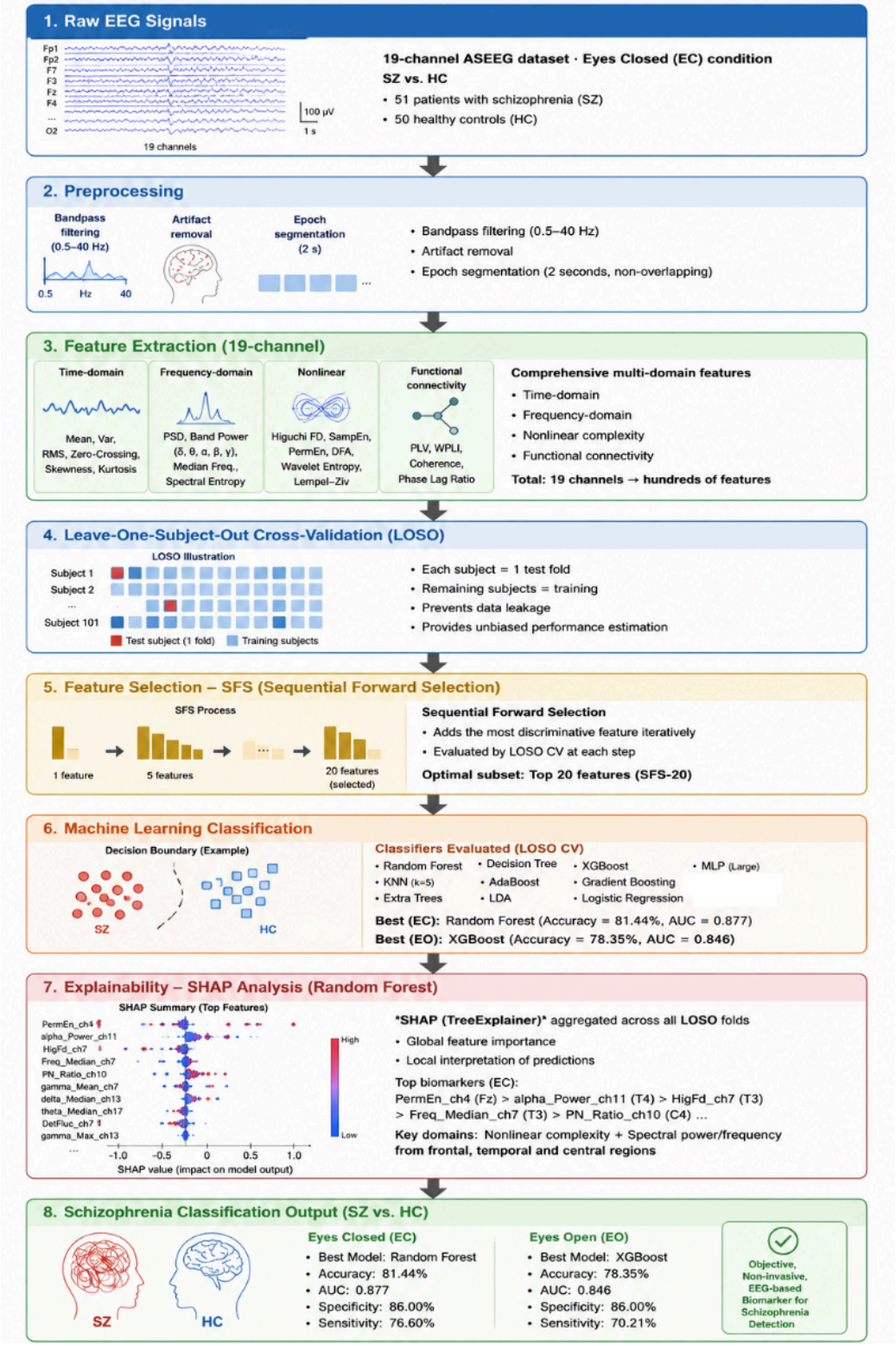


Figure 4

Overview of the proposed EEG-based schizophrenia classification framework. Resting-state EEG signals from the 19-channel ASEEG dataset were preprocessed, followed by multi-domain feature extraction. SFS identified the optimal 20-feature subset, and ten machine learning classifiers were evaluated using LOSO CV. SHAP applied to interpret the Random Forest model and identify the most influential EEG biomarkers for schizophrenia classification.